A Cas12a Toolbox for Rapid and Flexible Group B *Streptococcus* Genomic Editing and CRISPRi

Hillebrand GH[1], Carlin SC[2], Giacobe EJ[1], Stephenson HA[3], Collins J[4], Hooven TA[1,2,5,*]

Affiliations:

1. Program in Microbiology and Immunology, University of Pittsburgh School of Medicine, Pittsburgh PA, USA
2. Department of Pediatrics, Division of Newborn Medicine, University of Pittsburgh School of Medicine, Pittsburgh PA, USA
3. Dietrich School of Arts and Sciences, University of Pittsburgh, Pittsburgh PA, USA
4. Department of Microbiology and Immunology, School of Medicine, University of Louisville, Louisville KY, USA
5. RK Mellon Institute for Pediatric Research, Pittsburgh PA, USA

* Corresponding author:

Children's Hospital of Pittsburgh
Rangos Research Building
4401 Penn Ave., RRB #8128
Pittsburgh, PA 15224
thomas.hooven@chp.edu

Keywords: Group B *Streptococcus*, genome editing, Cas12a, CRISPRi

Abstract

Streptococcus agalactiae (group B *Streptococcus*; GBS) is a leading cause of neonatal sepsis and meningitis. Despite advances in molecular microbiology, GBS genome engineering remains laborious due to inefficient mutagenesis protocols. Here, we report a versatile and rapid Cas12a-based toolkit for GBS genetic manipulation. We developed two shuttle plasmids—pGBSedit for genome editing and pGBScrispri for inducible CRISPR interference—derived from an *Enterococcus faecium* system and optimized for GBS. Using these tools, we achieved targeted gene insertions, markerless deletions, and efficient, template-free mutagenesis via alternative end-joining repair. Furthermore, a catalytically inactive dCas12a variant enabled inducible gene silencing, with strand-specific targeting effects. The system demonstrated broad applicability across multiple GBS strains and minimal off-target activity, as confirmed by whole-genome sequencing. This Cas12a-based platform offers a rapid, flexible, and scalable approach to genetic studies in GBS, facilitating functional genomics and accelerating pathogenesis research.

40 Background:

41 *Streptococcus agalactiae* (group B *Streptococcus*; GBS) is a cause of severe
42 infections, particularly among perinatal populations: pregnant women, newborns, and
43 infants[1,2]. Genetic research is key to the development of GBS vaccines and targeted
44 therapeutics[3–5].

45 Currently, most protocols for GBS mutagenesis are based on temperature-
46 dependent shuttle plasmids[6,7]. The process for using a temperature-sensitive mutagenesis
47 plasmid begins with recombinant insertion of an editing cassette with flanking GBS
48 homologous sequences. After transformation into GBS, targeted plasmid integration into
49 the circular chromosome can be promoted by transitioning the culture to a temperature
50 that restricts extrachromosomal plasmid replication[6,8]. In a subsequent self-excision step,
51 the targeted region of the chromosome undergoes a second recombination event in which
52 the native sequence is replaced by the mutagenesis cassette originally introduced on the
53 plasmid[7].

54 While temperature-sensitive plasmids have been used to generate many GBS
55 mutants, successful use of these techniques remains time-consuming and laborious. One
56 drawback is that—to propagate the mutagenesis plasmid during the initial cloning and
57 transformant outgrowth steps—the cultures must be maintained at low temperature
58 (usually 28°C), which slows bacterial growth and prolongs the experimental timeframe.
59 Another problem is that the multiple passaging and outgrowth steps create opportunities
60 for unintended recombination and spontaneous mutation to occur. The result is that, even
61 when using a counterselection-optimized mutagenesis plasmid, it can take weeks or

62 months to create a single targeted GBS mutation. When unexpected problems arise, often
63 the only remedy is to return to the first step of the process, which delays progress.
64 Mutagenesis approaches based on the activity of clustered regularly interspaced
65 short palindromic repeats and CRISPR-associated protein (CRISPR/Cas) have
66 revolutionized genetic and molecular biology research[9–11]. Multiple CRISPR/Cas system
67 variants evolved in bacteria as defense mechanisms against exogenous, bacteriophage-
68 encoded DNA[12,13]. Bioengineered CRISPR/Cas systems have become useful as easily
69 programmable, targeted molecular effectors of numerous experimental functions
70 including flexible genome editing[14].
71 Techniques for using CRISPR/Cas for bacterial genome editing have proven
72 effective[15–18]. However, these efforts can be complicated by the presence of one or more
73 native CRISPR/Cas system encoded on the genome of the study species. In 2023, we
74 introduced a system for using a catalytically inactive dCas9 variant, encoded on the
75 chromosome of bioengineered mutant GBS strains, to downregulate gene expression
76 through CRISPR interference (CRISPRi)[19]. We also made multiple unreported, unsuccessful
77 efforts to use the native GBS CRISPR/Cas system to drive an effective genome editing
78 approach.
79 An alternative approach to bacterial genome editing is through introduction of non-
80 native bioengineered CRISPR/Cas systems. Cas12a (also referred to as Cpf1) is a type V-A
81 endonuclease found in class 2 CRISPR/Cas systems. Cas12a accepts a smaller guide RNA
82 (gRNA) than Cas9, and unlike the latter, Cas12a gRNA does not require presence of a trans-
83 activating CRISPR RNA (tracrRNA) for programmable targeting of specific DNA

84 sequences[18,20–23]. This allows for smaller, simpler plasmid-based platforms for Cas12a
85 introduction into new experimental systems. Cas12a requires a T-rich protospacer-
86 adjacent motif (PAM) to cleave a target sequence, which makes it an appealing choice for
87 use in low-GC organisms such as GBS[21].

88 Recent successful development of a Cas12a-based system for genome editing in
89 *Enterococcus faecalis* prompted us to examine its potential use in GBS[24]. Here we report
90 development, testing, and optimization of a single-plasmid Cas12a-based suite of GBS
91 genetic tools. We have used our Cas12a system for allelic exchange mutagenesis,
92 alternative end-joining mutagenesis, and targeted CRISPRi gene knockdown using a
93 catalytically deactivated Cas12a (dCas12a) variant. Our strategy is efficient. Using it, we
94 have made numerous mutants in an approximately one-week timeframe. Another
95 advantage over other GBS genetic tools (such as our dCas9-based CRISPRi technique) is
96 that it can be used across different GBS strain lineages with no requirement for preceding
97 alterations to the native chromosome. In summary, we find that using Cas12a for site-
98 directed GBS mutagenesis and genetic expression modulation is a significant improvement
99 over previously described techniques.

100

101 Results

102 *Chromosomal insertion of an eGFP expression cassette using Cas12a and*
103 *homology-directed repair.* **Figure 1** diagrams the design and potential uses of the two
104 plasmids that underpin our suite of Cas12a-based GBS genetic tools. pGBSedit is designed
105 for genome editing, while pGBScrispri is for CRISPRi. Both plasmids are modified versions

106 of the Cas12a-based shuttle plasmid pJC005, which was previously developed for *E.*
107 *faecium* genetic modification[24]. pGBSedit and pGBScrispri both encode conserved gram-
108 negative and gram-positive origins of replication so that CRISPR RNA (crRNA) and
109 homology arm cloning can be performed in *Escherichia coli* followed by electroporation
110 transformation of purified plasmid into GBS.

111 pGBSedit encodes WT *Acidaminococcus* Cas12a whereas pGBScrispri encodes a
112 modified, catalytically inactive (E993A) dCas12a that can be used for inducible, targeted
113 gene repression. In both versions of the plasmid, the *cas12a*/*dcas12a* gene is downstream
114 of a $P_{xyl/tet}$ inducible promoter bioengineered to maximize the dynamic range in response to
115 its anhydrotetracycline (aTC) inducer, with minimal expression in the uninduced state and
116 strong expression upon aTC exposure[25]. TetR, the promoter's repressor, is constitutively
117 expressed on the plasmid.

118 The crRNA cassette is identical in pGBSedit and pGBScripsri. Driven by a
119 constitutive P3 small RNA-optimized promoter, the crRNA region harbors a pair of apposed
120 *Esp3I* restriction enzyme cut sites that, when digested, yield incompatible sticky ends into
121 which a custom dsDNA spacer sequence be ligated to encode a functional crRNA-bearing
122 gRNA.

123 Once an active crRNA is cloned into place, with genomic target site
124 complementarity adjacent to a Cas12a PAM, aTC induction of WT *cas12a* from pGBSedit
125 leads to reliable selection against all GBS cells bearing the target sequence-PAM
126 combination. The only viable CFU are those that escaped selection by mutation of the
127 target site.

128 One experimentally useful mechanism of chromosomal repair is homologous
129 recombination with an editing template that can be cloned onto the pGBSedit plasmid at a
130 *XhoI* restriction enzyme recognition site downstream of the crRNA cassette. To
131 demonstrate the effectiveness of this approach, we created an editing template in which
132 the *eGFP* gene and a P23 constitutive promoter is flanked by approximately 500-nt
133 homology arms that direct it to an intergenic region conserved in CNCTC 10/84 and A909
134 GBS strains.
135 After cloning this editing template into pGBSedit, along with a targeting crRNA
136 directed to the intended genomic insertion site (generating pGBSedit:eGFP1, **Fig. 2A**), we
137 transformed WT CNCTC 10/84 and A909 with the targeting plasmid. In the uninduced state
138 without aTC, a liquid culture of the transformed GBS strain grew as an unselected lawn on
139 solid agar media (**Fig. 2B-C, left side**). However, when exposed to aTC added atop the agar
140 media, there is dramatic and reliable selection against the WT background that comprises
141 most of the lawn (**Fig. 2B-C, right side**). The only colonies that grew from the induced
142 CNCTC A909+pGBSedit:eGFP1 and 10/84+pGBSedit:eGFP1 populations expressed eGFP
143 genotypically (**Fig. 2D-E**) and phenotypically (**Fig. 2F-G**).
144
145 *Markerless gene deletion using Cas12a homology-directed repair.* An anticipated
146 use of the Cas12a tools in GBS is markerless gene (or other genomic region) deletion. To
147 demonstrate feasibility of this application and to quantify various possible Cas12a
148 selection endpoints, we created pGBSedit:Δ*covR1* to create a markerless deletion of the
149 *covR* gene. CovR is part of the two-component signaling system that regulates numerous

150 GBS genes[26,27] , including the *cyl* operon responsible for the biosynthetic pathway of β-
151 hemolysin/cytolysin (βHC), a pigmented, hemolytic GBS toxin[28,29]. We chose this target
152 gene because its deletion leads to *cyl* de-repression and an easily assayed
153 hyperpigmented, hyperhemolytic phenotype[30].

154 pGBSedit:Δ*covR1* has an anti-*covR* targeting crRNA directed to the target sequence
155 next to the 3'-TTTC PAM at nucleotide position 436 in the *covR* gene. In the pGBSedit *XhoI*
156 site, we cloned an approximately 1000-bp editing template composed of fused *CovR*
157 upstream and downstream homology arms (**Fig. 3A**).

158 After transformation of purified pGBSedit:Δ*covR1* into WT A909, we performed 14
159 independent aTC selection experiments during which we quantified the unselected
160 background CFU concentration and the aTC selection output. The mean rate of selection
161 escape across our 14 biological replicates was 1.1×10^{-4} (range 1×10^{-5} – 3.5×10^{-4}, **Fig.**
162 **3B**). We performed colony PCR on colonies from 8 independent biological replicates of the
163 transformation step. Among the 55 PCR reactions that generated an electrophoresis gel
164 band, 15 (27%) were of the expected size for the in-frame gene deletion, while the
165 remaining were consistent with wild type (**Fig. 3C**). Inspection of the 15 suspected
166 knockouts showed that all had the expected hyperpigmented appearance when grown in
167 liquid culture (**Fig. 3D**). To confirm that the knockout strain was hyperhemolytic, we
168 performed three biological replicates of hemolysis assays with one of the genotypic
169 knockouts from our experiment, which confirmed the expected phenotype (**Fig. 3E**).
170

171 *CRISPR/Cas12a GBS mutagenesis by recombinant free end repair*. To examine
172 whether Cas12a-mediated mutations at the genomic target site occur in the absence of
173 homologous recombination with an editing cassette, we generated *covR* and *eGFP*
174 targeting versions of pGBSedit without homology-based editing templates.
175 pGBSedit:*covR2* and pGBSedit:*eGFP2* target the *covR* and *eGFP* coding sequences,
176 respectively; pGBSedit:P23 targets the P23 promoter upstream of *eGFP* (**Fig. 4A-B**). We
177 transformed WT A909 with pGBSedit:*covR2* and A909 with chromosomal eGFP (A909eGFP)
178 with pGBSedit:*eGFP2* or pGBSedit:P23. After selection with aTC, we examined the surviving
179 colonies for phenotypic changes, noting that the majority of the WT A909+pGBSedit:*covR2*
180 colonies were hyperpigmented and hyperhemolytic and the A909eGFP+pGBSedit:*eGFP2*
181 and A909eGFP+pGBSedit:P23 colonies were not fluorescent. We performed colony PCR of
182 the genomic regions flanking the three Cas12a target sites, then Sanger sequenced the
183 resulting bands. This analysis identified two genomic deletions surrounding the Cas12a
184 targeted sites in the *covR* targeted colonies (**Fig. 4C**). One deletion was 2 bp in size and the
185 other was 60 bp. Sanger sequencing revealed one genomic deletion each for the P23
186 promoter and *eGFP* targeted strains (**Figs. 4D**). Predictably, mutations that delete
187 significant portions of the P23 promoter and coding sequence frameshift mutations lead to
188 loss of gene function in phenotypic testing (**Fig 4E-F**).
189 While the mutations that emerge from this template-less CRISPR editing approach
190 are unpredictably sized, we find that the speed and ease with which they can be generated
191 make this an attractive protocol for rapid creation of mutants in regions of interest. In our
192 benchmarking experiments, the full pipeline of crRNA cloning, GBS transformation and aTC

193 selection, and PCR/Sanger sequence confirmation could all be completed in a week.
194 Promising genomic changes made through this approach can then be more rigorously
195 verified by markerless deletion or allelic exchange with an editing template.
196
197 *Whole-genome sequencing of Cas12a-edited GBS genomes does not indicate*
198 *substantial off-target activity.* A persistent concern with CRISPR-based genomic editing is
199 the potential for off-target mutagenesis. Cas12 editing systems has been shown to have
200 promiscuous nickase activity[31] that could drive higher than baseline rates of mutation if
201 erroneous repair mechanisms were widely activated. To investigate this possibility, we
202 performed Illumina whole-genome sequencing of mutant strains recovered and tested in
203 the above experiments. After unbiased *de novo* alignment and contig scaffolding against a
204 reference GBS genome, we identified between 2 and 9 SNPs across our sequenced mutant
205 strain genomes. Additionally, a prophage resident in the A909 genome was observed to
206 have excised in one of our sequenced strains, which we have encountered in previous
207 studies unrelated to Cas12a mutagenesis[19]. Given estimated secular mutation rates in GBS
208 of approximately 10^{-9} mutations per bp per generation[32–35], or approximately 0.002
209 mutations per 2M-bp genome per generation, and roughly 20 generations per laboratory
210 outgrowth, 2-9 fixed SNPs in a strain that is 5-10 outgrowth steps from its progenitor roughly
211 matches expectations, and does not indicate widespread or biased off-site mutagenesis
212 activity by Cas12a.
213

214 *Inducible gene silencing with dCas12a*. To explore the potential of using dCas12a as
215 a tool for inducible gene silencing, we used crRNA targeting βHC biosynthetic enzymes
216 encoded by the *cyl* operon and crRNA targeting *covR* (**Fig. 5A**). Previous studies of
217 dCas12a-based gene silencing have demonstrated strand bias in which crRNA targeting
218 the template strand of the gene have a stronger silencing effect than crRNA targeting the
219 non-template strand[36]. This is the opposite of dCas9 gene silencing, which works best
220 when the non-template strand is targeted by the guide RNA (dCas9 template strand
221 targeting can actually increase gene expression in some cases)[19,37]. To examine this aspect
222 in our system, we used both template and non-template targeting crRNA.
223 We transformed CNCTC 10/84 with pGBScrispri:*cylx42* (template targeting) and
224 pGBScrispri:*cylx143* (non-template targeting). CNCTC 10/84 is a naturally
225 hyperpigmented/hyperhemolytic GBS strain, due to a SNP in the *covR* promoter that
226 results in constitutively low expression[38], so suppressing *cyl* in this background is expected
227 to reduce pigmentation and cytotoxicity. By qRT-PCR (**Fig. 5B**) and *in vitro* hemolysis assays
228 (**Fig. 5C**), we observed *cyl* downregulation in the presence of the aTC inducer and a
229 targeting crRNA. Addition of aTC without a targeting protospacer was noted to cause a
230 small but consistent upregulation of *cyl* expression, both by qRT-PCR and phenotypic
231 assay. As previously described, the template strand targeting pGBScrispri:*cylx42* plasmid
232 led to greater gene repression than the non-template targeting pGBScrispri:*cylx143* variant.
233 Silencing *covR* in A909, which is not a naturally hyperhemolytic strain, is expected to
234 cause *cyl* de-repression (**Fig. 5D**) and overexpression of the βHC toxin. Again, this expected
235 result was observed by qRT-PCR (**Fig. 5E**) and hemolysis assays (**Fig. 5F**), only in the

236 presence of the aTC inducer. (In contrast to CNCTC 10/84, aTC did not measurably increase
237 βHC expression in A909 when no *covR* targeting crRNA present, see **Fig. 5F** leftmost two
238 columns). Together, these results demonstrate the utility of inducible dCas12a as a rapid
239 and reliable tool for targeted gene expression knockdown in GBS.
240
241 Discussion
242 We have described a suite of Cas12a-based molecular tools to facilitate genetic
243 experiments in GBS. While Cas9-based platforms have dominated the first decade of
244 widespread CRISPR/Cas mediated biology, other Cas variants have been found to be
245 superior in some circumstances. The type V-A Cas12a enzyme, variants of which were first
246 characterized in *Acidaminococcus* spp. and *Lachnospiraceae* spp., generates staggered
247 DNA cleavage ends 18 nt (on the crRNA homologous strand) and 23 nt (on the crRNA
248 complementary strand) from the PAM[21]. This is different from Cas9, which generates blunt-
249 end double-stranded DNA cleavage[12]. Also distinct from Cas9 are the location and
250 sequence requirements of the Cas12a PAM. Whereas Cas9 uses a 5' PAM, which in most
251 *Streptococci* has a 5'-NGG sequence requirement, Cas12a recognizes 3'-TTTV upstream of
252 the target sequence.
253 Two major advantages of Cas12a-based technology for altering the GBS genome or
254 gene expression are that 1) the necessary Cas12a molecular components can be encoded
255 on a smaller plasmid than Cas9-based systems, making the cloning and GBS
256 transformation steps more likely to succeed; 2) because of significant structural
257 differences between Cas12a and Cas9, the native GBS CRISPR/Cas9 system has no

258 crosstalk with exogenously introduced Cas12a molecules. Leveraging these two important
259 advantages has allowed us to develop a set of efficient, inexpensive tools for rapid GBS
260 genetic experimentation. The resources described here should allow investigators to
261 choose from several complementary approaches for GBS chromosomal manipulation.

262 The dCas12a-based CRISPRi system is effective for inducible targeted gene
263 knockdown, as demonstrated by our successful downregulation of the *cyl* operon and the
264 *covR* gene that encodes a key transcriptional regulator of *cyl* and its expression of the
265 hemolytic toxin β/HC. In experiments with our recently published dCas9-based CRISPRi
266 system, we have shown that CRISPRi efficacy is variable[19]. Targeting dCas9 to the 5' end of
267 a protein-coding gene generally has a greater knockdown effect than targeting closer to the
268 3' gene terminus, but even different protospacers directing dCas9 to the first half of a
269 protein coding sequence can cause variable decreases in gene expression. We expect
270 similar findings with dCas12a-based CRISPRi and recommend that—whenever possible—
271 researchers examining gene function with dCas12a employ multiple different protospacers
272 targeting their gene of interest to boost the odds of maximizing the knockdown effect with
273 one of them.

274 The capabilities around direct chromosomal mutagenesis afforded by our system
275 open new possibilities in terms of speed and ease of generating new genetic variants. The
276 protocol for using a crRNA-only plasmid construct to generate variable end-joining
277 mutations at the target site can be completed in a week, which is a significant advance
278 over temperature-based plasmid selection/counter-selection systems. The recombinant
279 DNA mechanism underlying this end-joining mutagenesis phenomenon is not fully clear.

280 CRISPR/Cas-based genome editing in eukaryotic cells can make use of non-homologous
281 end-joining (NHEJ) mechanisms, but the enzymatic systems responsible for NHEJ are not
282 present in bacteria. Mechanistically simpler NHEJ processes, which depend on ATP-
283 dependent ligase-D and Ku enzymes, exist in *Mycobacteria* and *Bacillus* species, but are
284 not encoded by GBS[39–41].

285 A different bacterial double-stranded break repair pathway, known as alternative
286 end-joining (A-EJ) appears more likely to be functioning in the repair-driven mutagenesis we
287 observe in GBS following chromosomal Cas12a targeting[42,43]. A-EJ is a process of
288 microhomology-based DNA recombination. First described in *E. coli*, A-EJ of bacterial
289 chromosomal breaks is partially dependent on the RecBCD complex driving free end
290 degradation, leading eventually to exposure of compatible microhomologous sequences
291 (approximately 3-nt on average) that drive initial re-synapsis of apposing ends, followed by
292 gap repair. Because of the initial bidirectional free end degradation that underpins A-EJ, the
293 mutations left behind in the process reveal short or long sequence deletions eventually
294 resolved by stochastic microhomology-driven reannealing of the two free ends. Small
295 single-stranded gaps left over after microhomology synapsis are suspected to be repaired
296 by the essential enzyme LigA, followed by resolution of ssDNA flaps by 3' exonucleases or
297 SbcCD[44]. Because targeted Cas12a-initiated A-EJ creates variable, often frameshifted
298 chromosomal deletions, it can be harnessed as a tool for bioengineering experimental
299 mutations in GBS as we have shown here. A predicted mechanism for GBS A-EJ is
300 diagrammed in **Supplemental Fig. S1**.

301 Cas12a selection against WT chromosomal sequences can also be used to screen
302 for allelic exchange events generated by homology-driven recombination with an editing
303 template cloned into the same pGBSedit plasmid that carries the Cas12a and gRNA coding
304 sequences. This approach mirrors widely used CRISPR/Cas genome editing strategies that
305 have been effectively harnessed for studies on organisms across the tree of life. We have
306 successfully used Cas12a allelic exchange mutagenesis to replace genes with antibiotic
307 resistance markers, generate markerless gene deletions and SNPs, and insert new
308 sequences at specific sites on the chromosome.
309 This work highlights the value of flexible tool design when working in genetically
310 diverse species like GBS. The pGBSedit and pGBScrispri plasmids were constructed with
311 modular components that facilitate rapid adaptation to different experimental aims,
312 whether targeting chromosomal loci for allelic exchange or downregulating gene
313 expression through inducible repression. Because these tools do not rely on prior genomic
314 alterations, they are well-suited to applications across strain backgrounds and
315 experimental conditions.
316 Although this system streamlines many aspects of mutagenesis and gene regulation
317 in GBS, certain limitations remain. As with other CRISPR-based systems, off-target effects
318 cannot be entirely ruled out. Our tetracycline-inducible Cas12a system allows suppression
319 of the enzyme until a temporary exposure drives selection against the target (wild type)
320 genetic sequence, limiting the duration of susceptibility to Cas12a off-target effects.
321 Accordingly, our whole-genome sequencing results for the mutants we generated in this
322 study did not suggest indiscriminate mutagenesis from widespread Cas12a nickase

activity. However, the possibility of unintended mutations remains; whole-genome sequencing or complementary genetic controls are therefore advisable when feasible. In addition, while the ease of using end-joining mutagenesis is appealing, its reliance on stochastic microhomology limits its precision, and it may not be appropriate for applications requiring tightly defined genomic edits.

In summary, the Cas12a-based genetic toolkit presented here provides a set of versatile, efficient alternatives to more cumbersome traditional methods for GBS manipulation. By supporting targeted mutagenesis, promoter knockdown, and recombination-driven genome editing, these tools may facilitate broader efforts to interrogate GBS gene function and pathogenesis. We anticipate that their continued refinement and use will help advance genetic research in this clinically important organism.

Methods

Ethics statement: Whole blood collection by phlebotomy of healthy adult volunteers was conducted in accordance with an approved University of Pittsburgh IRB protocol (CR19110106-001). Following use of blood in GBS hemolysis assays, samples were discarded and no further volunteer-level data were collected.

Reagents: LB liquid broth mix, LB agar, TS liquid broth mix, TS agar, erythromycin, anhydrotetracycline, M17 liquid medium mix, glycine, *Esp3I*, T4 ligase, T4 polynucleotide

345 kinase, *XhoI*, Gibson assembly master mix, *DpnI*, Q5 Taq polymerase, Qiagen QIAprep Spin
346 Miniprep Kit, M17 broth, PEG6000
347
348 *Bacterial strains and growth conditions*: GBS strains A909 (serotype Ia, sequence
349 type 7) and CNCTC 10/84 (serotype V, sequence type 26), both of which were originally
350 isolated from infected neonates[38,45,46], and their derivatives were grown at 37°C under
351 stationary conditions in tryptic soy (TS) medium (Fisher Scientific cat. # DF0370-17-d). GBS
352 was supplemented with 5 μg/mL erythromycin as needed for selection. *E. coli* strain DH5α
353 was grown at 37°C with shaking in Luria-Bertani (LB) medium (Fisher Scientific cat. #
354 DF9446-07-5) supplemented with 300 μg/mL erythromycin as needed for selection.
355
356 *Statistical analyses*: Statistical analyses were performed with GraphPad Prism v.
357 10.2.3 for macOS.
358
359 *Construction of pGBSedit and pGBScrispi*: Plasmid backbone pJC005 was used as a
360 backbone for pGBSedit and pGBScrispri. A modular protospacer expression cassette with
361 a small RNA promoter (P3) driving the expression of the repeats and *Esp3I* editable sham
362 protospacer was added to both vectors. Digestion with *Esp3I* allows for complete removal
363 of the sham protospacer and ligation of new protospacers as annealed DNA oligos with
364 matching sticky ends. A unique *XhoI* cut site was also added at the end of this cassette for
365 linearization of the plasmid in use with Gibson Assembly addition of homology arms. This

366 modular cloning cassette was designed and ordered as a gene fragment from Twist
367 Bioscience added to both vectors via Gibson assembly.
368
369 *Protospacer design and insertion*: Cas12a-compatible GBS genomic target sites
370 with TTTV PAM sequences were identified with the aid of the CRISPick server hosted by the
371 Broad Institute[47]. Under the "CRISPRko/AsCas12a" settings, CRISPick generates a ranked
372 list of 23-nt sgRNA candidate sequences that interface correctly with our GBS Cas12a
373 tools. For dCas12a CRISPRi, sgRNA sequences complementary to the plus-strand should
374 be selected; for Cas12a mutagenesis, plus- or minus-strand sgRNA sequences are equally
375 effective.
376 After selecting a sgRNA target, the 23-nt sequence can be used to design custom
377 ssDNA protospacer sequences that can be annealed into a dsDNA cassette for cloning into
378 digested pGBSedit or pGBScrispri. The forward oligo is constructed as [TAGAT + sgRNA + A]
379 and the reverse oligo is constructed as [AAATT + reverse complement sgRNA + A]. These
380 ssDNA oligo constructs can be ordered separately from a synthetic DNA provider.
381 Purified pGBSedit (or pGBScrispri) plasmid, prepared from *E. coli* liquid culture is
382 digested with *Esp3I* according to manufacturer instructions, then the linearized plasmid is
383 gel extracted from an agarose electrophoresis gel.
384 The forward and reverse protospacer oligonucleotide samples are end-
385 phosphorylated then annealed as follows: rehydration of lyophilized samples to 100 μM
386 stocks then admixture of 1 μL forward oligo, 1 μL reverse oligo, 2.5 μL 10x T4 ligase buffer,
387 0.5 μL T4 Polynucleotide kinase, 20 μL ultrapure H_2O. Incubate at 37°C for 1 hour. After this

388 incubation, add 2.5 µL sterile 1 M NaCl, then heat the mixture to 95 °C in a heat block for 5
389 minutes. After this denaturation step, remove the heat block and allow it to cool slowly to
390 4°C with the oligo mixture tube remaining inserted in place.

391 Once phosphorylated and annealed, the dsDNA protospacer can be ligated into
392 *Esp3I*-digested, gel-purified pGBSedit/crispr plasmid in a 20 µL reaction containing 5 µL
393 *Esp3I*-digested plasmid; 2 µL phosphorylated/annealed protospacer; 2 µL 10x T4 ligase
394 buffer, 1 µL T4 ligase, 9 µL H_2O. Allow this reaction mixture to incubate at 16 °C for at least
395 two hours (overnight incubation is acceptable).

396 We use 5 µL of this ligation reaction to transform chemically competent *E. coli*.
397 Colony screening by PCR or sequencing-based methods can be used to confirm
398 appropriate protospacer insertion. We perform colony PCR using the forward ssDNA oligo
399 and pGBSedit_crRNA_Screen_R (GCTATCTTCGTCATAGTTACCT).

400

401 *Editing template design and insertion:* Editing templates included homology arms
402 with approximately 500 bp of overlap (on each end of the intended deletion or insertion).
403 The Cas12a target site, determined with the aid of CRISPick, was positioned roughly
404 equidistant from the homology arms. Editing constructs were ordered as synthesized gene
405 fragments but could alternatively be generated through recombinant techniques
406 depending on the intended end-use. We cloned the editing construct into linearized *XhoI*-
407 digested pGBSedit using Gibson assembly and used PCR and Sanger or whole-plasmid
408 sequencing techniques to verify the insert.

409 An alternative approach is to synthesize a gene fragment that contains the sgRNA
410 protospacer sequence and an editing template. Such a fragment can be quickly and fully
411 customized. For cloning of a gene fragment into pGBSedit, we use GeneFrag Insert Fwd
412 (GCAATAAAACTTATTCGGATCCGTCGTTTTACAACGTC) and GeneFrag Insert Rev
413 (AGCTGACGGTCAGAGAGAAAGGATTTCTCACATAAAATAGAGG) to linearize pGBSedit using
414 Q5 Taq polymerase. The PCR product can then be treated with *DpnI* to digest circular
415 plasmid, followed by gel or column purification of the PCR reaction mixture. We designed
416 custom gene fragments with homology arms that enable Gibson assembly insertion into
417 linearized pGBSedit, then confirmed proper cloning by whole-plasmid sequencing.
418
419 *Plasmid purification and transformation into GBS:* Once cloning products had been
420 sequence-confirmed in *E. coli*, plasmids were purified using the Qiagen QIAprep Spin
421 Miniprep Kit according to manufacturer instructions.
422 Electrocompetent GBS was prepared by seeding a 30 mL culture of M17 broth+
423 0.5% glucose (GM17) with a single colony from an overnight agar plate and allowing
424 overnight growth at 37 °C. The next morning, the overnight culture was added to 200 mL of
425 GM17 supplemented with 2% glycine and pre-warmed to 37 °C. The culture growing in
426 glycine-containing broth was monitored until it reached an $O.D._{600}$=0.6. The culture was
427 then pelleted and washed twice in ice-cold 10% polyethylene glycol (average molecular
428 weight=6000; PEG6000), then washed again and the entire pellet resuspended in 25 mL of
429 ice-cold PEG6000 wash solution containing supplemental 25% glycerol. 50 µL aliquots of
430 this suspension were then used for electroporation transformation of the purified shuttle

431 plasmid, followed by overnight outgrowth on selective agar plates, as previously described
432 [7].
433
434 *Outgrowth and selection for homology-driven recombination mutants:* Following
435 GBS transformation with an editing plasmid, a single colony was resuspended in 20 µL 1x
436 phosphate buffered saline (PBS). 2 µL of this resuspension was used as template for a
437 colony PCR reaction to confirm presence of the intended plasmid. Simultaneously, the
438 remaining 18 µL of the PBS-resuspended sample was seeded into a 10 mL
439 TS+erythromycin 5 µg/mL culture, which was allowed to grow stationary at 37 °C for 6-8
440 hours.
441 Following this 6-8-hour outgrowth, 1:10 and 1:100 dilutions of the culture were
442 prepared (dilute in TS+erythromycin). 150 µL of the following cultures were then plated on
443 separate TS+erythromycin 5 µg/mL agar plates: undiluted, 1:10, and 1:100, undiluted+aTC,
444 1:10+aTC, and 1:100+aTC. For the aTC-containing cultures for plating, we add 6 µL of a 2
445 mg/mL aTC stock to the 150 µL of sample being plated (for ease, the aTC stock can be
446 added directly into the pooled plating sample on the agar, then the mixture sterilely spread
447 across the surface).
448 These plates are then allowed to grow for 36 hours at 37 °C. A multiple-log fold
449 difference between colony counts on the aTC and non-aTC plates after growth is indicative
450 of successful Cas12a selection against wild-type GBS. At least 8 colonies are selected and
451 each resuspended in 20 µL 1x PBS. 2 µL of this resuspension is used in a colony PCR
452 reaction to access genotype. Simultaneously, the remaining 18 µL of the PBS-resuspended

453 sample was plated for single colonies on a TS+erythromycin 5 µg/mL plate. Colonies with
454 desired genotype by colony PCR are chosen. Using an isolated colony from the plate struck
455 for single colonies, resuspend a colony in 20 µL 1x PBS and use 2 µL of this resuspension in
456 a second confirmatory colony PCR of genotype. Once confirmed, purify PCR product from
457 gel for sanger sequencing and seed remain 18 µL of colony resuspension into a 40 mL TS
458 broth culture to begin plasmid curing.
459
460 *Outgrowth and selection for free end joining mutants*: To use pGBSedit, without an
461 editing cassette, to generate free end joining mutants, the same experimental procedures
462 are followed as with generation of a homology-driven recombination mutant. However,
463 because free end joining mutants can be the result of indels that are too small for easy
464 detection by comparing PCR bands on an electrophoresis gel, we first perform a colony
465 PCR screen on approximately 16 colonies, checking for the presence or absence of the wild
466 type Cas12a target (the sequence complementary to the pGBSedit protospacer). We use
467 the target site as the forward PCR primer and choose a reverse primer approximately 500
468 kB downstream. From this screen, we select candidate colonies that do not generate
469 bands. These are the candidate mutant strains. Then we perform a second colony PCR
470 reaction on the candidate mutant strains, using forward and reverse primers approximately
471 500 kB from the target site in each direction. Colonies that yield bands on this second
472 reaction can be genotyped using Sanger sequencing of the amplicon or whole genome
473 sequencing to identify and characterize free end joining mutations..
474

475 *CFU quantification of Cas12 selective force (Fig 3B):* 14 individual TS+5 µg/mL
476 erythromycin cultures were inoculated using GBS harboring the pGBSedit CovR Deletion
477 plasmid and grown for 8 hours. Serial dilutions and CFU plating on TS+5 µg/mL
478 erythromycin plates for each overnight culture were performed to access total viable
479 CFU/mL. Simultaneously, 100 µL of each overnight culture was plated onto TS+5 µg/mL
480 erythromycin+500 ng/mL aTC at both 1:10 or 1:100 dilutions. After 36 hours growth, CFU
481 counts on aTC plates were taken and compared to total number of viable CFU plated from
482 the starting culture
483
484 *Measurement of Mutagenesis frequency (Fig 3C):* pGBSedit CovR Deletion plasmid
485 was transformed into electrocompetent GBS in 6 biological replicates. 1 colony from each
486 transformation was grown and aTC selected per previously reported method. 16 colonies
487 from each of the 6 biological replicates were selected and screened for genotypes by NEB
488 OneTaq colony PCR (Cat. M0482L). Genotypes were counted based by 1% agarose gel
489 electrophoresis PCR band sizes (3048 bp WT and 2358 bp covR KO).
490
491 *Colony PCR*: Colony PCR reactions were performed using NEB OneTaq Master Mix
492 (Cat. M0482L) and custom-prepared ssDNA oligonucleotide primers. Wild type isogenic
493 GBS colonies were used as positive control samples; sterile water was used as template in
494 negative control samples. All templates for reactions are colonies that were first
495 resuspended in 1xPBS. Manufacturer instructions were followed, including proper
496 calculation of primer annealing temperatures and PCR extension time.

497

498 *Outgrowth and induction of knockdown strains:* GBS harboring the pGBScrispri
499 plasmid are grown in TS broth supplemented with 5 µg/mL erythromycin to maintenance
500 the plasmid. For phenotypic assays, induction of knockdown is achieved by the addition of
501 250 ng/mL anhydrotetracycline (stock 2 mg/mL in water) at inoculation. Cultures
502 inoculated from isolated single colonies. Cultures are grown stationary at 37°C for 18
503 hours.

504

505 *pGBSedit plasmid curing from confirmed mutants*: 40 mL TS broth cultures were
506 inoculated using an isolated colony that has been genotypically confirmed and grown
507 stationary at 37°C overnight. A second passage in 40 mL of TS broth is performed using 100
508 µL of previous culture as inoculum. 1:10,000 and 1:100,000 dilutions of the grown second
509 passage were plated on TS agar plates. 8 colonies selected were dual patched onto TS and
510 TS+5 µg/mL Erm agar plates to identify antibiotic sensitivity.

511

512 *Fluorescence assay:* 10 mL TS broth cultures were inoculated using an isolated
513 colony and grown overnight at 37°C shaking. Shaking cultures were used to ensure oxygen
514 is present during maturation of GFP chromophore formation. Overnight cultures were spun
515 at 4000rpm for 5 minutes and washed twice with PBS before being OD600 normalized to 1
516 in PBS. 10 mL of OD600 normalized cultures were spun down at 4000rpm for 5 minutes and
517 resuspended in 1 mL of PBS to 10x concentrate. 200 µL of each sample was loaded in

518 technical triplicate into a black optical bottom 96-well plate. GFP was excited at 488 nm
519 and emission was observed at 515 nm with a 515 nm filter.
520
521 *RNA purification and qRT-PCR:* 10 mL TS+5 µg/mL erythromycin broth cultures were
522 inoculated using an isolated colony and grown to mid-log (OD600 of 0.6) before being split
523 into two 5 mL cultures; not treated and 250 ng/mL anhydrotetracycline supplemented.
524 Cultures were incubated at 37°C for 1 hour post treatment before being spun down at
525 4000rpm for 5 minutes and resuspended in 1 mL of RNAprotect Bacterial Reagent (Qiagen
526 Catalogue: 76506). Bacteria were incubated in RNAprotect at room temperature for 5
527 minutes before being pelleted in microcentrifuge tubes at 15,000rpm for 2 minutes. Excess
528 RNAprotect was removed and pellets were frozen and held at -80°C until RNA extraction.
529 RNA protected pellets were thawed on ice and RNA was extracted using the Qiagen RNeasy
530 Kit (Cat. 74104) per manufacturer protocol. RNA was eluted with warmed (95°C)ultra-pure
531 water in place of elution buffer. DNA was removed with Invitrogen DNA-free Kit (Cat.
532 AM1906) per manufacturer protocol. cDNA was made with AppliedBiosytems High-
533 Capacity cDNA Reverse Transcription Kit (Cat. 4374966) per manufacturer protocol. cDNA
534 and reverse transcription negative were 1:10 diluted with ultra-pure water before 1 µL was
535 used as template in 10 µL qPCR reactions. Bio Rad SsoAdvanced Universal SYBR Green
536 Supermix (Cat. 1725272) was used for all qPCR reactions.
537
538 *Hemolysis assays:* 10 mL of human whole blood was donated, heparinized and
539 spun down for 10 minutes at 2000 rpm. Serum was removed with a serological pipette and

540 5 mL of Hanks buffers saline solution (HBSS) is added to the packed red blood cells via
541 inversion. Packed red blood cells (RBC) were spun for 10 minutes at 2000rpm and the
542 supernatant was removed with a serological pipette. 500uL of packed RBCs were added to
543 50 mL of HBSS to achieve a 1% packed RBC solution. 10 mL cultures of GBS harboring the
544 pGBScrispri plasmid were grown in TS broth supplemented with 5 µg/mL erythromycin and
545 either with or without 250 ng/mL of anhydrotetracycline. Cultures were grown stationary at
546 37°C for 18 hours. Cultures were pelleted at 4000rpm and resuspended in 10 mL of PBS to
547 wash. 10 mL PBS resuspensions were OD600 normalized to 1 using a cuvette. 10 mL of OD
548 normalized A909 cultures were concentrated 10x to an OD600 of 10 by pelleting and
549 resuspending in 1 mL of PBS. 10/84 cultures were 1:10 diluted in PBS after OD
550 normalization. Hemolysis assays were performed with 100 µL of 1% packed RBCs and 100
551 µL of bacterial suspension incubated at 37°C for either 15 minutes (10/84) or 1 hour (A909).
552 Hemolysis assays were performed in 96 well V-bottom plates and in technical triplicate.
553 After hemolysis, V-bottom plates were spun down at 2000rpm for 2 minutes and
554 supernatants (100 µL) were collected for each sample and absorbance at 415 nm was used
555 to measure released hemoglobin in the supernatant. Percent hemolysis is calculated
556 relative to a 1% triton control.
557
558 *Whole-genome sequencing, scaffolding, and analysis.* Genomic DNA samples were
559 prepared for whole-genome sequencing (WGS) using the Illumina DNA Prep tagmentation
560 kit with IDT for Illumina Unique Dual Indexes. Sequencing was performed on an Illumina
561 NextSeq2000 platform with a 300-cycle flow cell to generate paired-end reads (2x150 bp).

562 A 1-2% PhiX control library was included to ensure optimal base-calling accuracy. Initial
563 processing—including demultiplexing, read trimming, and analytics—was performed using
564 Illumina DRAGEN software (version 3.10.12)[48]. Quality control included FastQC metrics
565 evaluation.

566 Further processing and genomic assembly utilized a custom bioinformatics
567 pipeline. Reads underwent stringent quality filtering, trimming, and duplicate grouping
568 using BBTools. Filtered reads were aligned to the A909 GBS strain reference genome to
569 create a high-confidence consensus sequence, requiring a minimum depth of 10 reads at
570 consensus sites.

571 Reads were assembled into contigs using SPAdes[49] in careful mode. Contigs were
572 scaffolded onto the consensus reference using RagTag[50] , followed by patching to resolve
573 scaffold gaps and inconsistencies. The primary scaffold from each assembly was extracted
574 and annotated using the Prokaryotic Genome Annotation Pipeline (PGAP)[51]. Pipeline scripts
575 and dependencies were managed within a custom conda environment and run locally.

576

577 *Conflicts of interest:* The authors have no conflicts of interest to declare.

578

579 *Acknowledgements*: This work was supported by the National Institutes of Health (NIH)
580 R21AI178067, R01AI182835, and R01AI177991 (T.A.H.), a UPMC Children's Hospital of
581 Pittsburgh Research Advisory Council graduate student grant (G.H.H.), and Centers of
582 Biomedical Research Excellence (CoBRE) Grant P20GM125504 (J.C.). Figure panels
583 throughout were generated using BioRender.

584

585 Figure Captions

586

587 **Figure 1. Design and workflow of the Cas12a-based GBS genetic toolkit.** Plasmid maps
588 and workflows of the Cas12a-based genetic toolkit for Group B Streptococcus. The two
589 shuttle vectors—pGBSedit (encoding wild-type Cas12a) and pGBScrispri (encoding
590 catalytically inactive dCas12a)—carry a $P_{xyl/tet}$-inducible promoter upstream of the
591 cas12a/dcas12a gene, a constitutive TetR repressor, and an *Esp3I*-flanked protospacer
592 insertion site; pGBSedit also includes a unique *XhoI* site for cloning homology arms. Three
593 experimental protocols are illustrated: (1) homology-directed repair mutagenesis, in which
594 an editing template directs precise genomic insertions or deletions followed by
595 anhydrotetracycline (aTC) selection; (2) template-less mutagenesis, where Cas12a-
596 induced double-strand breaks are repaired via the native alternative end-joining pathway
597 to generate variable indels; and (3) inducible CRISPR interference, in which dCas12a
598 binding to the target locus upon aTC induction leads to targeted gene knockdown.

599 **Figure 2. Cas12a-mediated insertion of eGFP into the GBS chromosome via homology-**
600 **directed repair.**
601 (A) Diagram of pGBSedit:eGFP1, with ~500-nt upstream and downstream homology arms
602 flanking the *eGFP* coding sequence targeted to an intergenic locus conserved in A909 and
603 CNCTC 10/84.
604 (B & C) Representative agar plates of A909 (B) and CNCTC 10/84 (C) transformants on

605 erythromycin: without aTC (left) showing unselected background, and with 500 ng/mL aTC

606 (right) showing only *eGFP* integrants.

607 (D & E) Colony PCR of aTC-selected colonies: expected band sizes for WT (upper) and

608 eGFP insertion (lower) indicated.

609 (F & G) Fluorescence imaging under blue-light illumination confirming *eGFP* expression in

610 selected A909 (G) and CNCTC 10/84 resuspended colonies.

611 **Figure 3. Markerless deletion of covR using Cas12a homology-directed repair.**

612 (A) Design of pGBSedit:ΔcovR1, containing fused ~1 kb homology arms upstream and

613 downstream of the *covR* coding sequence.

614 (B) Selection escape frequency for ΔcovR1 across 14 independent aTC selections in A909;

615 each symbol represents one biological replicate, and the horizontal bar denotes the mean

616 (1.1×10^{-4}).

617 (C) Genotyping by colony PCR of 55 aTC-selected colonies from six biological replicates;

618 27% yielded the expected ΔcovR amplicon.

619 (D) Photograph of liquid cultures showing hyperpigmented phenotype of confirmed ΔcovR

620 mutants.

621 (E) Quantification of hemolytic activity for Δ*covR* versus WT, measured by released

622 hemoglobin absorbance (n = 3; mean ± SD).

623

624 **Figure 4. CRISPR/Cas12a-mediated free end-joining mutagenesis in GBS.**

625 (A & B) Plasmid designs for template-less mutagenesis: pGBSedit:covR2, pGBSedit:eGFP2,

626 and pGBSedit:P23, each encoding a protospacer targeting covR, chromosomal eGFP, or
627 the P23 promoter.
628 (C) Representative sequence alignments from covR2 mutants showing a 2-bp deletion and
629 a 60-bp deletion at the target site. Microhomology regions suspected to have served as loci
630 for alternative end-joining are boxed.
631 (D) Indel patterns at the P23 and eGFP protospacer sites in selected mutants.
632 Microhomology regions suspected to have served as loci for alternative end-joining are
633 boxed.
634 (E) Hyperhemolytic phenotype of *covR* mutants in a hemolysis assay (n=3; mean ± SD).
635 (F) Loss of eGFP fluorescence in *eGFP2* mutants and reduced P23 promoter activity in P23
636 mutants.
637

638 **Figure 5. Inducible gene silencing in GBS using dCas12a CRISPR interference.**
639 (A) Protospacer designs for dCas12a targeting: cylx42 (template strand) and cylx143 (non-
640 template strand) in the *cyl* operon, and a *covR*-targeting protospacer.
641 (B) qRT-PCR quantification of *cyl* expression in CNCTC 10/84 with (+ aTC) or without (–
642 aTC) induction (n = 3; mean ± SD), showing stronger knockdown with template-strand
643 targeting.
644 (C) Hemolysis assays of CNCTC 10/84 strains demonstrating reduced βHC activity upon
645 dCas12a targeting of *cyl* (mean ± SD; n = 3).
646 (D) qRT-PCR of *cyl* expression in A909 harboring *covR*-targeting dCas12a, showing de-
647 repression upon induction (n = 3; mean ± SD).

648 (E) Hemolysis assays of A909 *covR* knockdown strain confirming increased βHC activity

649 with aTC induction (mean ± SD; n = 3).

650 Supplemental materials

651 **Supplemental Figure S1:** Proposed mechanism of alternative end-joining in GBS.

652 **Supplemental Extended Protocol**: Detailed instructions for using pGBSedit and

653 pGBScrispri.

654 Public resources availability

655 The following plasmids for GBS Cas12a editing, CRISPRi, and complementation are

656 available at Addgene.

657

Addgene Plasmid Number	Plasmid Name
223200	pGBSedit Sham
223201	pGBScrispri Sham
223202	pGBScomp High

223203	pGBScomp Low

References

1. Lawn JE, Bianchi-Jassir F, Russell NJ, Kohli-Lynch M, Tann CJ, Hall J, Madrid L, Baker CJ, Bartlett L, Cutland C, Gravett MG, Heath PT, Ip M, Doare KL, Madhi SA, Rubens CE, Saha SK, Schrag S, Meulen AS ter, Vekemans J, Seale AC. Group B Streptococcal Disease Worldwide for Pregnant Women, Stillbirths, and Children: Why, What, and How to Undertake Estimates? Clin Infect Dis. 2017;65(suppl_2):S89–S99. PMID: 29117323

2. Gonçalves BP, Procter SR, Paul P, Chandna J, Lewin A, Seedat F, Koukounari A, Dangor Z, Leahy S, Santhanam S, John HB, Bramugy J, Bardají A, Abubakar A, Nasambu C, Libster R, Yanotti CS, Horváth-Puhó E, Sørensen HT, Beek D van de, Bijlsma MW, Gardner WM, Kassebaum N, Trotter C, Bassat Q, Madhi SA, Lambach P, Jit M, Lawn JE, outcomes GD and D collaborative group for long term, outcomes GL and MIC collaborative group for long term, sub-group GSAG epidemiological, team C, Søgaard KK, Kassel MN van, Snoek L, Gier B de, Ende A van der, Hahné SJM, Harden LM, Ghoor A, Mbatha S, Lowick S, Laughton B, Jaye T, Lala SG, Sithole P, Msayi J, Kumalo N, Msibi TN, Arumugam A, Murugesan N, Rajendraprasad N, Priya M, Mabrouk A, Katana PV, Mwangome E, Newton CR, Mucasse H, Aerts C, Massora S, Medina V, Rojas A, Amado D, Llapur CJ, Hossain AKMT, Rahman QS ur, Ip M, Seale A, Heath PT, Doare KL, Khalil A, Schrag SJ, Meulen AS ter, Mason E, Blau DM, Arifeen SE, Assefa N, Onyango D, Sow SO, Mandomando I, Ogbuanu I, Kotloff KL, Scott JAG, Gurley ES, Barr BAT, Mahtab S. Group B streptococcus infection during pregnancy and infancy: estimates of regional and global burden. Lancet Glob Heal. 2022;10(6):e807–e819. PMCID: PMC9090904

3. Patras KA, Nizet V. Group B Streptococcal Maternal Colonization and Neonatal Disease: Molecular Mechanisms and Preventative Approaches. Frontiers Pediatrics. 2018;6:27. PMCID: PMC5827363

4. Brokaw A, Furuta A, Dacanay M, Rajagopal L, Waldorf KMA. Bacterial and Host Determinants of Group B Streptococcal Vaginal Colonization and Ascending Infection in Pregnancy. Front Cell Infect Mi. 2021;11:720789.

5. Kobayashi M, Vekemans J, Baker CJ, Ratner AJ, Doare KL, Schrag SJ. Group B Streptococcus vaccine development: present status and future considerations, with emphasis on perspectives for low and middle income countries. F1000research. 2016;5:2355. PMID: 27803803

6. Yim HH, Rubens CE. Site-specific homologous recombination mutagenesis in group B streptococci. Methods Cell Sci. 1998;20(1–4):13–20.

7. Hooven TA, Bonakdar M, Chamby AB, Ratner AJ. A Counterselectable Sucrose Sensitivity Marker Permits Efficient and Flexible Mutagenesis in Streptococcus agalactiae. Appl Environ Microb. 2019;85(7). PMID: 30658970

8. Framson PE, Nittayajarn A, Merry J, Youngman P, Rubens CE. New genetic techniques for group B streptococci: high-efficiency transformation, maintenance of temperature-sensitive pWV01 plasmids, and mutagenesis with Tn917. Applied and environmental microbiology. 1997 Sep;63(9):3539 3547.

9. Mali P, Esvelt KM, Church GM. Cas9 as a versatile tool for engineering biology. Nat Methods. 2013;10(10):957–963. PMCID: PMC4051438

10. Doudna JA, Charpentier E. Genome editing. The new frontier of genome engineering with CRISPR-Cas9. Science. 2014 Nov 28;346(6213):1258096. PMID: 25430774

11. Jinek M, Chylinski K, Fonfara I, Hauer M, Doudna JA, Charpentier E. A Programmable Dual-RNA–Guided DNA Endonuclease in Adaptive Bacterial Immunity. Science. 2012;337(6096):816–821. PMID: 22745249

12. Chen JS, Doudna JA. The chemistry of Cas9 and its CRISPR colleagues. Nat Rev Chem. 2017;1(10):0078.

13. Murugan K, Babu K, Sundaresan R, Rajan R, Sashital DG. The Revolution Continues: Newly Discovered Systems Expand the CRISPR-Cas Toolkit. Mol Cell. 2017;68(1):15–25. PMCID: PMC5683099

14. Pickar-Oliver A, Gersbach CA. The next generation of CRISPR–Cas technologies and applications. Nat Rev Mol Cell Bio. 2019;20(8):490–507. PMCID: PMC7079207

15. Kurushima J, Tomita H. Advances of genetic engineering in streptococci and enterococci. Microbiol Immunol. 2022; PMID: 35703039

16. Choi KR, Lee SY. CRISPR technologies for bacterial systems: Current achievements and future directions. Biotechnol Adv. 2016 Nov 15;34(7):1180 1209. PMID: 27566508

17. Oh JH, Pijkeren JP van. CRISPR-Cas9-assisted recombineering in Lactobacillus reuteri. Nucleic Acids Res. 2014;42(17):e131 e131. PMCID: PMC4176153

18. Jiang Y, Qian F, Yang J, Liu Y, Dong F, Xu C, Sun B, Chen B, Xu X, Li Y, Wang R, Yang S. CRISPR-Cpf1 assisted genome editing of Corynebacterium glutamicum. Nat Commun. 2017 May 4;8:15179. PMID: 28469274

19. Gopalakrishna KP, Hillebrand GH, Bhavana VH, Elder JL, D'Mello A, Tettelin H, Hooven TA. Group B Streptococcus Cas9 variants provide insight into programmable gene repression and CRISPR-Cas transcriptional effects. Commun Biol. 2023;6(1):620. PMCID: PMC10256743

20. Senthilnathan R, Ilangovan I, Kunale M, Easwaran N, Ramamoorthy S, Veeramuthu A, Muthukaliannan GK. An update on CRISPR-Cas12 as a versatile tool in genome editing. Mol Biol Rep. 2023;50(3):2865–2881. PMID: 36641494

21. Zetsche B, Gootenberg JS, Abudayyeh OO, Slaymaker IM, Makarova KS, Essletzbichler P, Volz SE, Joung J, van der Oost J, Regev A, Koonin EV, Zhang F. Cpf1 Is a Single RNA-Guided Endonuclease of a Class 2 CRISPR-Cas System. Cell. 2015;163(3):759–771. PMCID: PMC4638220

22. Yan MY, Yan HQ, Ren GX, Zhao JP, Guo XP, Sun YC. CRISPR-Cas12a-Assisted Recombineering in Bacteria. Appl Environ Microbiol. 2017;83(17):e00947-17. PMCID: PMC5561284

23. Meliawati M, Schilling C, Schmid J. Recent advances of Cas12a applications in bacteria. Appl Microbiol Biotechnol. 2021;105(8):2981–2990. PMCID: PMC8053165

24. Chua MJ, Collins J. Rapid, Efficient, and Cost-Effective Gene Editing of Enterococcus faecium with CRISPR-Cas12a. Microbiol Spectr. 2022;10(1):e02427-21. PMCID: PMC8809335

25. Helle L, Kull M, Mayer S, Marincola G, Zelder ME, Goerke C, Wolz C, Bertram R. Vectors for improved Tet repressor-dependent gradual gene induction or silencing in Staphylococcus aureus. Microbiology+. 2011 Nov 30;157(12):3314–3323. PMID: 21921101

26. Mazzuoli MV, Daunesse M, Varet H, Rosinski-Chupin I, Legendre R, Sismeiro O, Gominet M, Kaminski PA, Glaser P, Chica C, Trieu-Cuot P, Firon A. The CovR regulatory network drives the evolution of Group B Streptococcus virulence. Plos Genet. 2021;17(9):e1009761. PMCID: PMC8448333

27. Claverie C, Coppolino F, Mazzuoli MV, Guyonnet C, Jacquemet E, Legendre R, Sismeiro O, Gaetano GVD, Teti G, Trieu-Cuot P, Tazi A, Beninati C, Firon A. Constitutive activation of two-component systems reveals regulatory network interactions in Streptococcus agalactiae. Nat Commun. 2024;15(1):9175. PMCID: PMC11502775

28. Armistead B, Whidbey C, Iyer LM, Herrero-Foncubierta P, Quach P, Haidour A, Aravind L, Cuerva JM, Jaspan HB, Rajagopal L. The cyl Genes Reveal the Biosynthetic and Evolutionary Origins of the Group B Streptococcus Hemolytic Lipid, Granadaene. Front Microbiol. 2020;10:3123. PMCID: PMC6985545

29. Randis TM, Gelber SE, Hooven TA, Abellar RG, Akabas LH, Lewis EL, Walker LB, Byland LM, Nizet V, Ratner AJ. Group B Streptococcus β-hemolysin/Cytolysin Breaches Maternal-Fetal Barriers to Cause Preterm Birth and Intrauterine Fetal Demise in Vivo. J Infect Dis. 2014 Jul 15;210(2):265 273. PMCID: PMC4092248

30. Lupo A, Ruppen C, Hemphill A, Spellerberg B, Sendi P. Phenotypic and molecular characterization of hyperpigmented group B Streptococci. Int J Med Microbiol. 2014 Jul;304(5–6):717–724. PMID: 24933304

31. Murugan K, Seetharam AS, Severin AJ, Sashital DG. CRISPR-Cas12a has widespread off-target and dsDNA-nicking effects EDITORS' PICK: Cas12a nickase activities. J Biol Chem. 2020;295(17):5538–5553. PMCID: PMC7186167

32. Drake JW, Charlesworth B, Charlesworth D, Crow JF. Rates of Spontaneous Mutation. Genetics [Internet]. 1998;148(4):1667–1686. Available from: https://www.genetics.org/content/148/4/1667

33. Cuny C, Barretto C, Rosinski-Chupin I, Cunha VD, Domelier AS, Glaser P. Evolutionary rates and emergence of human-associated GBS lineages. Microbial Genomics. 2021;7(8):000486.

34. Rosinski-Chupin I, Sauvage E, Mairey B, Mangenot S, Ma L, Cunha VD, Rusniok C, Bouchier C, Barbe V, Glaser P. Reductive evolution in Streptococcus agalactiae and the emergence of a host adapted lineage. Bmc Genomics. 2013;14(1):252. PMCID: PMC3637634

35. Sheppard SK, Lees JA, Taylor B, al. et. Population genomics of Group B Streptococcus: global structure and adaptive evolution. Nature Communications. 2018;9(1):2460.

36. Zhang X, Wang J, Cheng Q, Zheng X, Zhao G, Wang J. Multiplex gene regulation by CRISPR-ddCpf1. Cell Discov. 2017;3(1):17018. PMCID: PMC5460296

37. Qi LS, Larson MH, Gilbert LA, Doudna JA, Weissman JS, Arkin AP, Lim WA. Repurposing CRISPR as an RNA-Guided Platform for Sequence-Specific Control of Gene Expression. Cell. 2013 Feb 28;152(5):1173 1183. PMCID: PMC3664290

38. Zhu L, Beres SB, Yerramilli P, Pruitt L, Cantu CC, Olsen RJ, Musser JM. Genetic Basis Underlying the Hyperhemolytic Phenotype of Streptococcus agalactiae Strain CNCTC10/84. J Bacteriol. 2020;202(23). PMCID: PMC7648153

39. Della M, Palmbos PL, Tseng HM, Tonkin LM, Daley JM, Topper LM, Pitcher RS, Tomkinson AE, Wilson TE, Doherty AJ. Mycobacterial Ku and Ligase Proteins Constitute a Two-Component NHEJ Repair Machine. Science. 2004;306(5696):683–685. PMID: 15499016

40. Weller GR, Kysela B, Roy R, Tonkin LM, Scanlan E, Della M, Devine SK, Day JP, Wilkinson A, Fagagna F d'Adda di, Devine KM, Bowater RP, Jeggo PA, Jackson SP, Doherty AJ. Identification of a DNA Nonhomologous End-Joining Complex in Bacteria. Science. 2002;297(5587):1686–1689. PMID: 12215643

41. Shuman S, Glickman MS. Bacterial DNA repair by non-homologous end joining. Nat Rev Microbiol. 2007;5(11):852–861. PMID: 17938628

42. Chayot R, Montagne B, Mazel D, Ricchetti M. An end-joining repair mechanism in Escherichia coli. Proc Natl Acad Sci. 2010;107(5):2141–2146. PMCID: PMC2836643

43. Hou Z, Yu T, Yi Q, Du Y, Zhou L, Zhao Y, Wu Y, Wu L, Wang T, Bian P. High-complexity of DNA double-strand breaks is key for alternative end-joining choice. Commun Biol. 2024;7(1):936. PMCID: PMC11297215

44. Lee J, Jo I, Ahn J, Hong S, Jeong S, Kwon A, Ha NC. Crystal structure of the nuclease and capping domain of SbcD from Staphylococcus aureus. J Microbiol. 2021;59(6):584–589. PMID: 33877576

45. Nizet V, Gibson RL, Chi EY, Framson PE, Hulse M, Rubens CE. Group B streptococcal beta-hemolysin expression is associated with injury of lung epithelial cells. Infection and Immunity. 1996 Sep;64(9):3818 3826.

46. Lancefield RC, McCarty M, Everly WN. Multiple mouse-protective antibodies directed against group B streptococci. Special reference to antibodies effective against protein antigens. J Exp Medicine. 1975;142(1):165–179. PMID: 1097573

47. Pedrozo CNN, Peralta TM, Olea FD, Locatelli P, Crottogini AJ, Belaich MN, Cuniberti LA. In silico performance analysis of web tools for CRISPRa sgRNA design in human genes. Comput Struct Biotechnol J. 2022;20:3779–3782. PMCID: PMC9304428

48. Behera S, Catreux S, Rossi M, Truong S, Huang Z, Ruehle M, Visvanath A, Parnaby G, Roddey C, Onuchic V, Cameron DL, English A, Mehtalia S, Han J, Mehio R, Sedlazeck FJ. Comprehensive and accurate genome analysis at scale using DRAGEN accelerated algorithms. bioRxiv. 2024;2024.01.02.573821. PMCID: PMC10802302

49. Bankevich A, Nurk S, Antipov D, Gurevich AA, Dvorkin M, Kulikov AS, Lesin VM, Nikolenko SI, Pham S, Prjibelski AD, Pyshkin AV, Sirotkin AV, Vyahhi N, Tesler G, Alekseyev MA, Pevzner PA. SPAdes: A New Genome Assembly Algorithm and Its Applications to Single-Cell Sequencing. J Comput Biol. 2012;19(5):455–477. PMCID: PMC3342519

50. Alonge M, Lebeigle L, Kirsche M, Jenike K, Ou S, Aganezov S, Wang X, Lippman ZB, Schatz MC, Soyk S. Automated assembly scaffolding using RagTag elevates a new tomato system for high-throughput genome editing. Genome Biol. 2022;23(1):258. PMCID: PMC9753292

51. Tatusova T, DiCuccio M, Badretdin A, Chetvernin V, Nawrocki EP, Zaslavsky L, Lomsadze A, Pruitt KD, Borodovsky M, Ostell J. NCBI prokaryotic genome annotation pipeline. Nucleic Acids Res. 2016;44(14):6614–6624. PMCID: PMC5001611

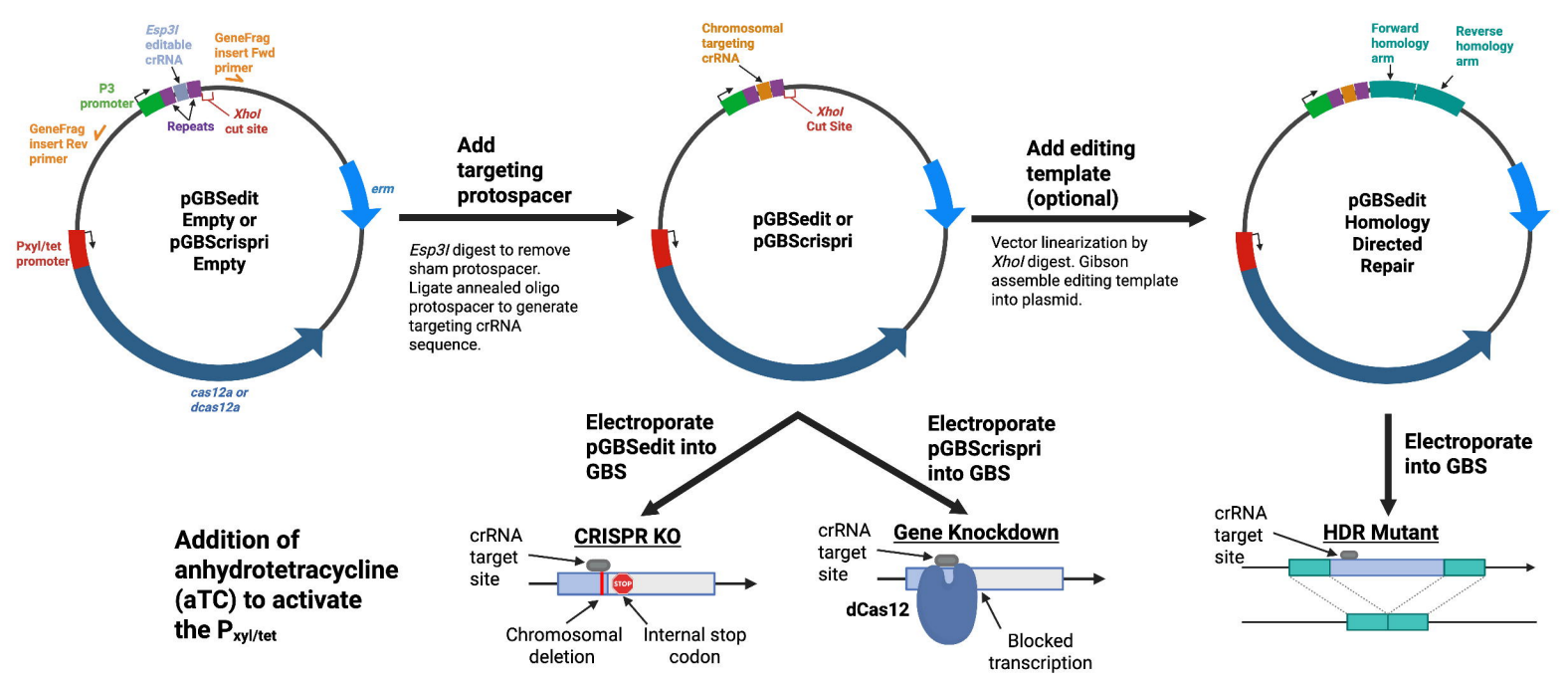
Esp3I editable crRNA
GeneFrag insert Fwd primer
P3 promoter
Repeats
XhoI cut site
GeneFrag insert Rev primer
pGBSedit Empty or pGBScrispri Empty
erm
Pxyl/tet promoter
cas12a or dcas12a
Add targeting protospacer
Esp3I digest to remove sham protospacer. Ligate annealed oligo protospacer to generate targeting crRNA sequence.
Chromosomal targeting crRNA
XhoI Cut Site
pGBSedit or pGBScrispri
Add editing template (optional)
Vector linearization by XhoI digest. Gibson assemble editing template into plasmid.
Forward homology arm
Reverse homology arm
pGBSedit Homology Directed Repair
Electroporate pGBSedit into GBS
Electroporate pGBScrispri into GBS
Electroporate into GBS
Addition of anhydrotetracycline (aTC) to activate the Pxyl/tet
crRNA target site
CRISPR KO
STOP
Chromosomal deletion
Internal stop codon
crRNA target site
Gene Knockdown
dCas12
Blocked transcription
crRNA target site
HDR Mutant

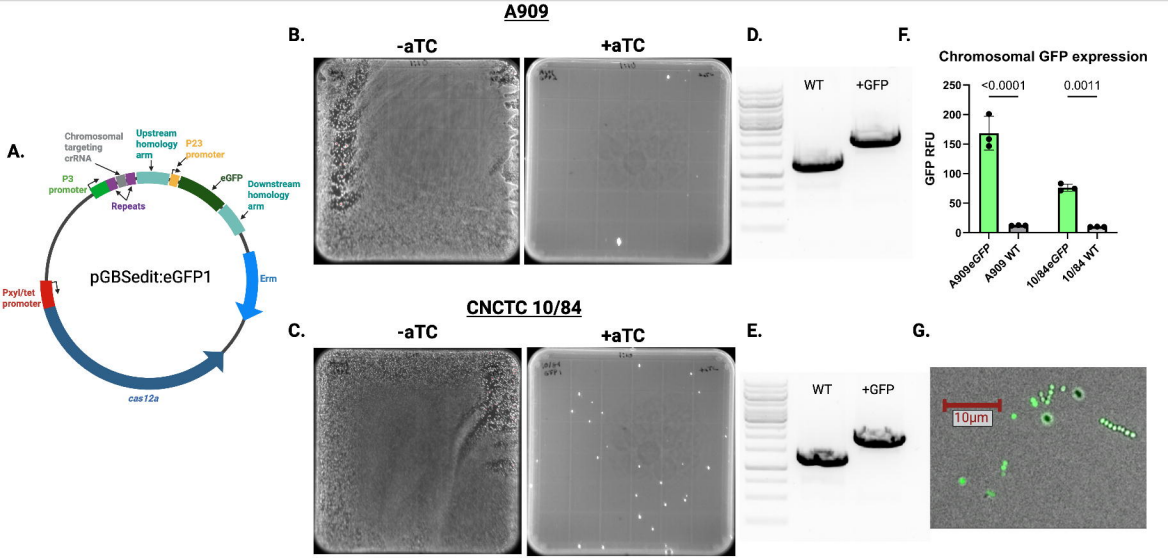
A909
A.
Chromosomal targeting crRNA
Upstream homology arm
P23 promoter
P3 promoter
eGFP
Repeats
Downstream homology arm
pGBSedit:eGFP1
Erm
Pxyl/tet promoter
cas12a
B.
-aTC
+aTC
C.
-aTC
+aTC
CNCTC 10/84
D.
WT
+GFP
E.
WT
+GFP
F.
Chromosomal GFP expression
<0.0001
0.0011
GFP RFU
250
200
150
100
50
0
A909eGFP
A909 WT
10/84eGFP
10/84 WT
G.
10µm

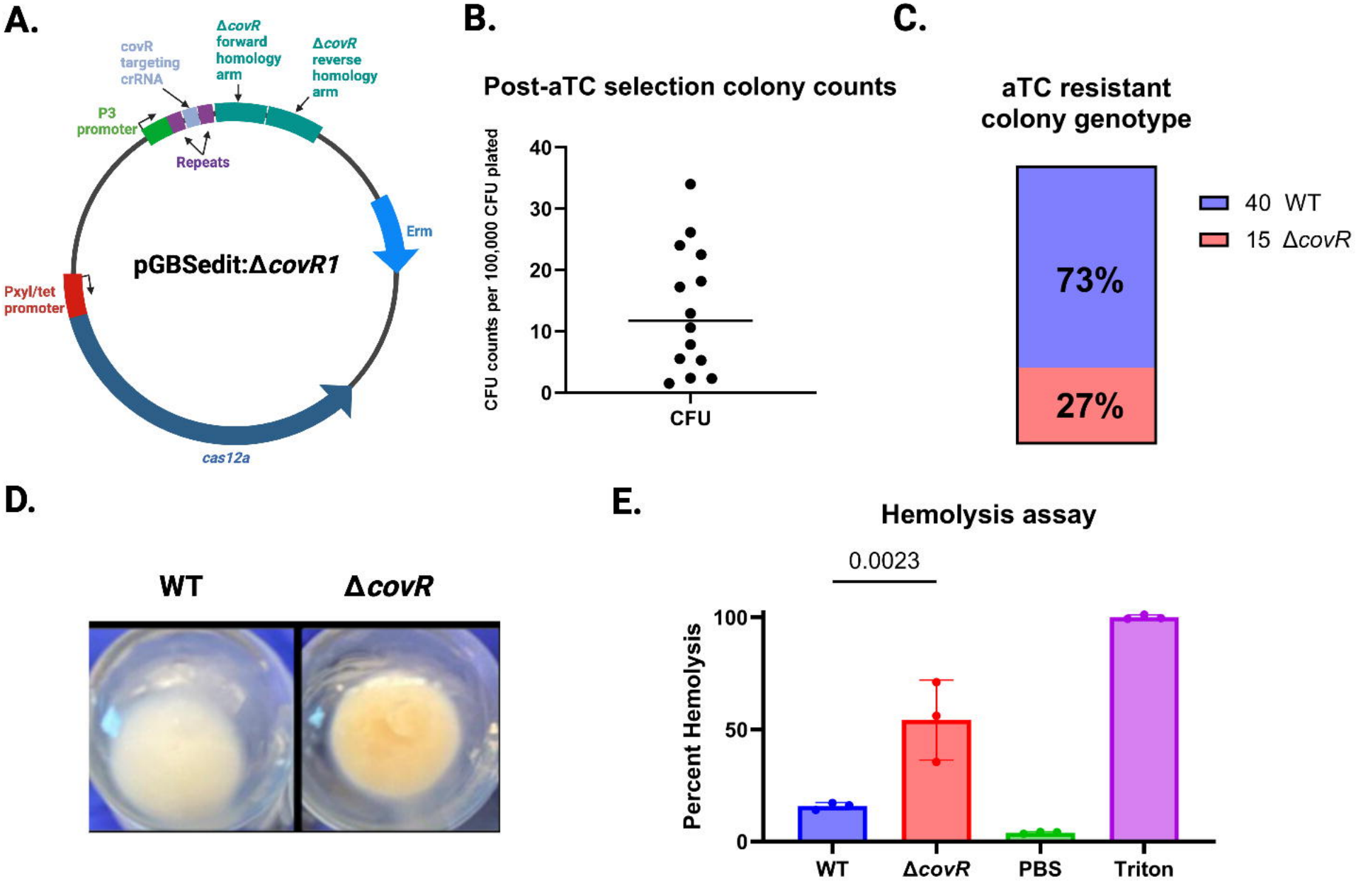
A.
covR targeting crRNA
ΔcovR forward homology arm
ΔcovR reverse homology arm
P3 promoter
Repeats
Erm
pGBSedit:ΔcovR1
Pxyl/tet promoter
cas12a
B.
Post-aTC selection colony counts
CFU counts per 100,000 CFU plated
40
30
20
10
0
CFU
C.
aTC resistant colony genotype
73%
27%
40 WT
15 ΔcovR
D.
WT
ΔcovR
E.
Hemolysis assay
0.0023
Percent Hemolysis
100
50
0
WT
ΔcovR
PBS
Triton

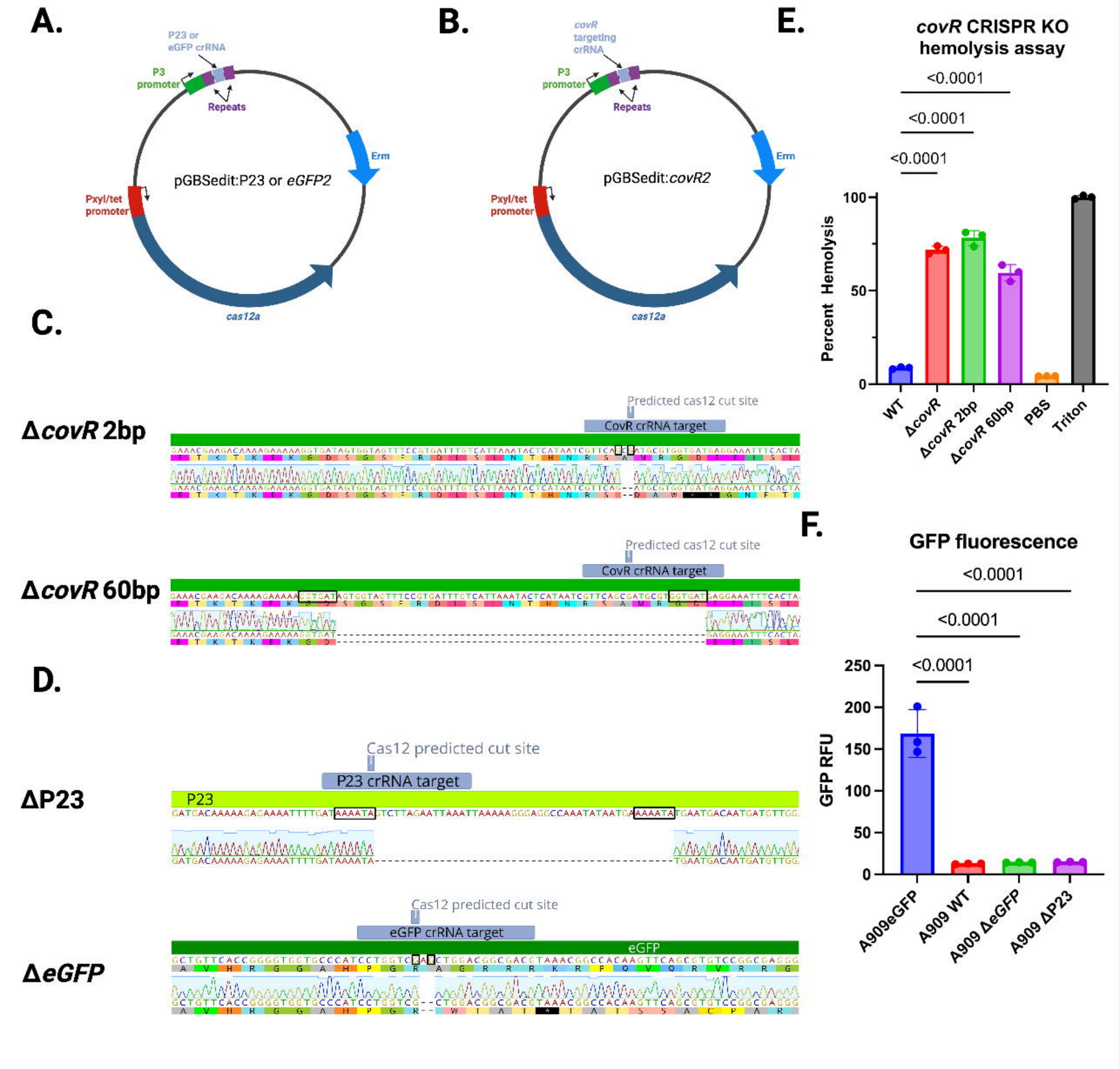
A.
P23 or eGFP crRNA
P3 promoter
Repeats
Erm
pGBSedit:P23 or eGFP2
Pxyl/tet promoter
cas12a
B.
covR targeting crRNA
P3 promoter
Repeats
Erm
pGBSedit:covR2
Pxyl/tet promoter
cas12a
E.
covR CRISPR KO hemolysis assay
<0.0001
<0.0001
<0.0001
Percent Hemolysis
100
50
0
WT
ΔcovR
ΔcovR 2bp
ΔcovR 60bp
PBS
Triton
C.
ΔcovR 2bp
Predicted cas12 cut site
CovR crRNA target
ΔcovR 60bp
Predicted cas12 cut site
CovR crRNA target
F.
GFP fluorescence
<0.0001
<0.0001
<0.0001
GFP RFU
250
200
150
100
50
0
A909eGFP
A909 WT
A909 ΔeGFP
A909 ΔP23
D.
ΔP23
Cas12 predicted cut site
P23 crRNA target
P23
ΔeGFP
Cas12 predicted cut site
eGFP crRNA target
eGFP

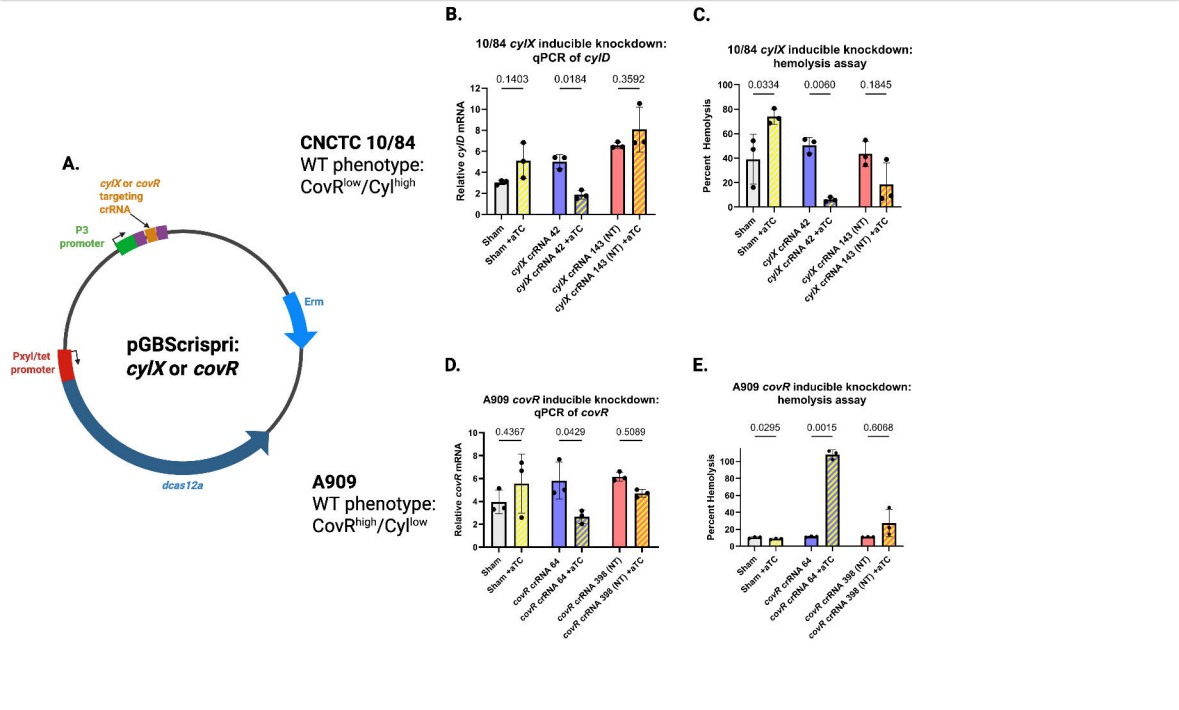
A.
cylX or covR targeting crRNA
P3 promoter
Erm
Pxyl/tet promoter
pGBScrispri: cylX or covR
dcas12a
CNCTC 10/84
WT phenotype:
CovR^low/Cyl^high
A909
WT phenotype:
CovR^high/Cyl^low
B.
10/84 cylX inducible knockdown: qPCR of cylD
Relative cylD mRNA
0.1403
0.0184
0.3592
Sham
Sham +aTC
cylX crRNA 42
cylX crRNA 42 +aTC
cylX crRNA 143 (NT)
cylX crRNA 143 (NT) +aTC
C.
10/84 cylX inducible knockdown: hemolysis assay
Percent Hemolysis
0.0334
0.0060
0.1845
D.
A909 covR inducible knockdown: qPCR of covR
Relative covR mRNA
0.4367
0.0429
0.5089
covR crRNA 64
covR crRNA 64 +aTC
covR crRNA 398 (NT)
covR crRNA 398 (NT) +aTC
E.
A909 covR inducible knockdown: hemolysis assay
Percent Hemolysis
0.0295
0.0015
0.6068

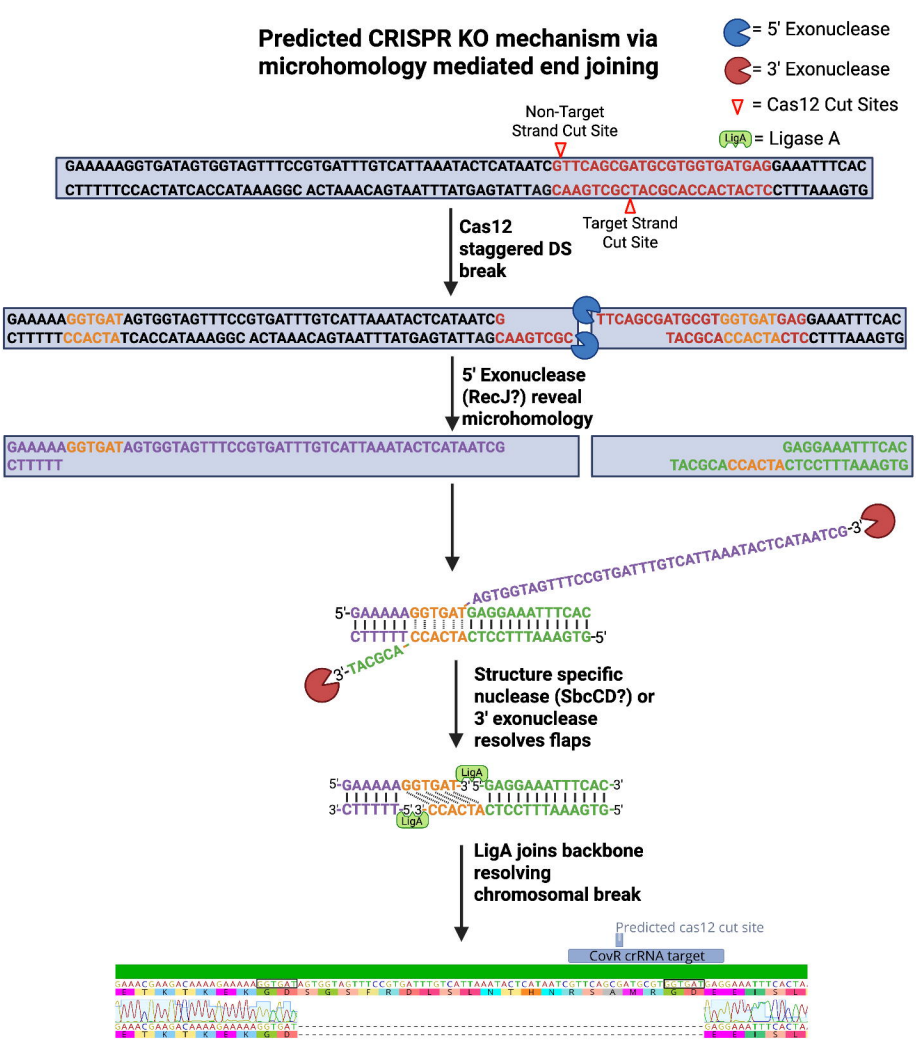
Predicted CRISPR KO mechanism via microhomology mediated end joining
= 5' Exonuclease
= 3' Exonuclease
= Cas12 Cut Sites
LigA = Ligase A
Non-Target Strand Cut Site
GAAAAAGGTGATAGTGGTAGTTTCCGTGATTTGTCATTAAATACTCATAATCGTTCAGCGATGCGTGGTGATGAGGAAATTTCAC
CTTTTTCCACTATCACCATAAAGGC ACTAAACAGTAATTTATGAGTATTAGCAAGTCGCTACGCACCACTACTCCTTTAAAGTG
Target Strand Cut Site
Cas12 staggered DS break
GAAAAAGGTGATAGTGGTAGTTTCCGTGATTTGTCATTAAATACTCATAATCG
TTCAGCGATGCGTGGTGATGAGGAAATTTCAC
CTTTTTCCACTATCACCATAAAGGC ACTAAACAGTAATTTATGAGTATTAG
TACGCACCACTACTCCTTTAAAGTG
5' Exonuclease (RecJ?) reveal microhomology
GAAAAAGGTGATAGTGGTAGTTTCCGTGATTTGTCATTAAATACTCATAATCG
CTTTTT
GAGGAAATTTCAC
TACGCACCACTACTCCTTTAAAGTG
AGTGGTAGTTTCCGTGATTTGTCATTAAATACTCATAATCG-3'
5'-GAAAAAGGTGATGAGGAAATTTCAC
CTTTTTCCACTACTCCTTTAAAGTG-5'
3'-TACGCA-
Structure specific nuclease (SbcCD?) or 3' exonuclease resolves flaps
LigA
5'-GAAAAAGGTGAT-3' 5'-GAGGAAATTTCAC-3'
3'-CTTTTT-5' 3'-CCACTACTCCTTTAAAGTG-5'
LigA
LigA joins backbone resolving chromosomal break
Predicted cas12 cut site
CovR crRNA target